

## Conductivity and gating of silicon ringchains

Joseph L. Speyer, Igor V. Ovchinnikov, Daniel Neuhauser,<sup>a)</sup> and Delroy Baugh  
*Department of Chemistry and Biochemistry, University of California-Los Angeles (UCLA), Los Angeles, California 90095-1569*

(Received 24 March 2005; accepted 2 August 2005; published online 23 September 2005)

One-dimensional and two-dimensional conductivity calculations are done for a set of several closely spaced quantum silicon rings, following the development of bottom-up approaches for producing silicon rings. The transmission is easily influenced by electric and magnetic gatings and has band features even for two or three rings, showing its potential usefulness for logical devices. Analysis on different gatings shows that the electric-field gating would be as effective as the Aharonov-Bohm magnetic gating. © 2005 American Institute of Physics. [DOI: [10.1063/1.2042454](https://doi.org/10.1063/1.2042454)]

### I. INTRODUCTION

Recently, Rose and Baugh introduced a new approach to the synthesis of nanostructure devices.<sup>1,2</sup> In their approach, a set of silicon rings is established by self-assembly methods. It is possible to synthesize either a single ring or several rings connected together, or even a host of different rings and structural arrays, e.g., linear, triangular, square arrays, etc. The rings can be precisely tuned to different sizes ranging in diameter from microns down to tens of nanometers and, in the future, hopefully smaller diameters. Furthermore, the rings can be connected directly by silicon bridges or left apart so that the electrons tunnel from one ring to another, with the tunneling amplitude dependent on the (tunable) ring-ring separation.

In this paper we pose the question on what would be the simplest quantum conductance properties of an assembly of such rings. These are expected to be very interesting since the ring diameters can be made smaller than the coherence length of electrons in silicon (which is less than 1  $\mu\text{m}$  at 2 K). Therefore, ring-based devices can show completely coherent transport, especially at low temperatures.

Even a single ring is interesting quantum mechanically.<sup>3-6</sup> It serves as a cavity, much like a Mach-Zender modulator. On the molecular level, rings were suggested as possible logic devices; in particular, this applies to molecules which are ringlike, such as para-connected naphthalene.<sup>7-9</sup> Magnetic-field effects on a single ring can also be used to influence conductivity.<sup>10</sup>

When we move up in size from molecular to nanometer-size rings,<sup>11</sup> such as those examined here, the experimental capabilities in terms of manufacturing and especially connecting these rings become much more advanced, making it realistic to imagine the use of rings for next-generation devices. Silicon rings,<sup>12</sup> in particular, could be easily placed with appropriate isolation with silicon on insulator<sup>13</sup> (SOI), and, with the new approaches suggested by Rose and Baugh,<sup>1,2</sup> could be manipulated precisely.

Most fundamentally, the use of silicon rings in the solid state opens the way for placing several rings together. This leads to several questions:

- What are the conductance properties of several rings in tandem, and even more importantly, how does gating affect such devices? Specifically, what effects do electric and magnetic fields have on ring devices?
- What would be the properties of 2D and possibly 3D collections of rings?
- How would a multilead ring respond to charging?

In this work we primarily concentrate on the first question. We do a simple one-dimensional- (1D) type simulation in which the silicon rings are represented by Huckel-type “strings,” as well as two-dimensional (2D) simulations of small rings. The simulations, while rudimentary, are sufficient to demonstrate several interesting properties of the rings. In particular, we will show that even two and especially three rings connected together show very sharp band edges reminiscent of a band structure in a periodic multiring system. The use of several rings has several advantages in that in a practical device the voltage drops along each ring would be reduced. This would reduce the possibility of excitation of optical phonons, which would raise the temperature and reduce the electron coherence, thereby degrading performance.

We also study in detail different approaches for gating, including magnetic gating (Aharonov-Bohm effect),<sup>10</sup> gating by constant potential, or gating by transverse potential, and show that they all lead to the same effect explained in a simple model.

The methodology is presented in Sec. II, followed by the results and discussion.

### II. METHODOLOGY

#### A. Huckel-type calculations

We first do a Huckel-type study in which we represent the rings by sites. [See Fig. 1(a).] The Huckel-type matrix elements are

<sup>a)</sup>Electronic mail: dxn@chem.ucla.edu

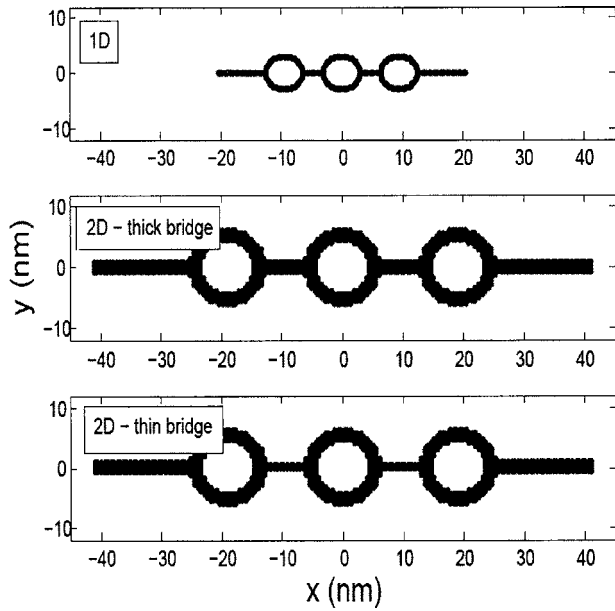


FIG. 1. Maps of the systems studied. The top graph refers to the 1D case, while the lower two refer to 2D. The middle graph refers to the system with a thick bridge (width 2.0 nm), while the bottom graph refers to the system with a thin bridge (width 1.0 nm).

$$H_{IJ} = \begin{cases} 2\beta + V(I), & I = J \\ -\beta + i\alpha B f(I, J) & \text{for } I, J \text{ physically connected,} \\ I \neq J, & \end{cases} \quad (1)$$

where

$$\beta = \frac{1}{2m\Delta^2}$$

is the kinetic coupling,  $m$  is the effective mass of the conducting electron (taken as  $0.25m_e$  here), and  $\Delta$  is the effective site-to-site distance. The distance is approximately 10 a.u., and this value was used as the grid spacing in 2D; for the 1D results to mimic the 2D ones, we needed, however, to take  $\Delta = 5$  a.u. so  $\beta \sim 0.08$  a.u.  $\sim 2$  eV.

Strictly saying, the Hamiltonian should also possess the diamagnetic part proportional to the square of the magnetic field. However, the diamagnetic field is small (less than 0.001 eV here) so that it would not affect the motion.

$V(I)$  is the voltage on each point in the devices. We examine both the cases of a gate voltage and a linearly varying voltage transverse to the main axis (i.e., along the  $y$  axis in the figure).

$f(I, J)$  is a matrix element of the angular momentum operator on the loop; it is  $R/\Delta$  if  $I$  and  $J$  are nearest neighbors within the rings and connected counterclockwise,  $-R/\Delta$  for clockwise connection within the rings, and 0 otherwise.  $B$  is the magnetic field,  $R$  is the loop radius ( $=3$  nm for the 1D Huckel simulations). For a field of, say, 10 Tesla, the off-diagonal element is 0.025 eV, or  $\sim 1\%$  of the size of the real part.

We apply the Huckel Hamiltonian for the shapes shown

in Fig. 1(a): a single ring, two rings, and three rings. The transmission conductivity is calculated by using the flux-flux formula with an absorbing potential,<sup>14</sup>

$$N(E) = 4 \text{Tr}(\Gamma_L G \Gamma_R G^\dagger),$$

where we introduced the absorbing potential on the left and the right of the leads, which are added to the Hamiltonian:<sup>15</sup>

$$G = \frac{1}{E - (H - i\Gamma_L - i\Gamma_R)}.$$

The simulations are converged with regard to the strength and width of the absorbing potential.

## B. Two-dimensional calculations

We have also done two-dimensional calculations, which are necessary because even though the motion along each wire segment of the ring is essentially one-dimensional, the curvature in any “fork” is expected to require a proper 2D simulation.

The structure of the system is shown in Figs. 1(b) and 1(c) (for a three-loop system, which includes up to 1056 grid points). Each ring had a diameter of 12 nm and a width of 2 nm, so that the width of the ring included at least four grid points on each side. This grid spacing is rough, but should be sufficient for describing the 2D effects.

The rings were connected by wires of varying width—either 1 nm (two grid points) or 2 nm (four grid points). Figure 1 shows [in addition to the 1D results, Fig. 1(a)] the system for thick [Fig. 1(b)] and thin [Fig. 1(c)] 2D wires.

The 2D simulations are done by a similar technique to the Huckel approach. Each point is connected to other points that have the same  $x$  or same  $y$  by a DVR formula:<sup>16</sup>

$$H(x, y, x', y') = \left( V(x, y) + \frac{\pi^2(dx^{-2} + dy^{-2})}{6m} \right) \delta_{xx'} \delta_{yy'} + \frac{\delta_{xx'}(-1)^{(y-y')/dy}}{2m(y-y')^2} + \frac{\delta_{yy'}(-1)^{(x-x')/dx}}{2m(x-x')^2},$$

where we introduced the constant grid spacing in  $x$  and  $y$ . The local potential is assumed to be infinite away from the loop-wire structure so that no grid points are taken in those areas; we place any gate potentials and the transverse potential on  $V(x, y)$ . Also, no magnetic-field effects were used in 2D.

The Hamiltonian, with absorbing potentials on the left and right leads, is diagonalized and the eigenvectors and eigenvalues are then used to calculate the flux-flux formula directly from the trace.

## III. SIMULATIONS

Figures 2–4 show the summed transmission coefficient,  $N(E)$ , as a function of the energy of the electron which is ejected into the system. [In an actual device,  $N(E)$  would measure the conductance for a small energy difference if the Fermi energy is  $E$ ]. All energies are measured in eVs. These figures show the progression of the results when one moves from one to two to three rings. Figure 2 shows the results for

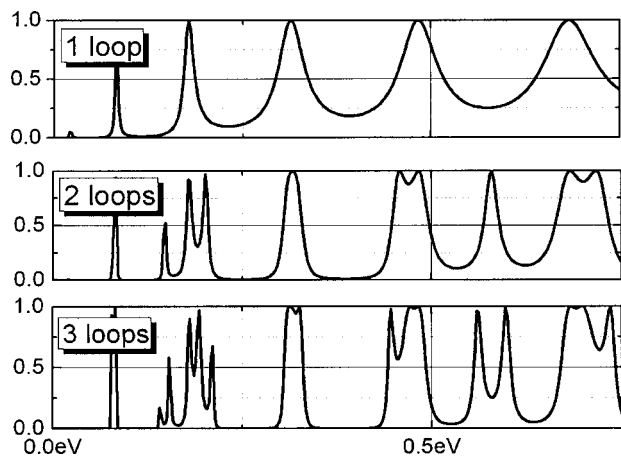


FIG. 2. Transmission vs energy for a 1D system and a varying number of loops.

the 1D system, Fig. 3 for the 2D system with the thick bridges, and Fig. 4 for the 2D system with the thin bridges.

The most interesting aspect of these runs is how quickly a band-structure-like behavior occurs, where the transitions from on to off are very sharp (for general discussion see, e.g., Ref. 17). The transition is very sharp in the 1D case, but is also quite strong (0%–100% transition) in the 2D case. Thus, it should be advantageous to fabricate devices connecting several rings.

Figures 5–7 shows the effects of a gating voltage perpendicular to the leads (i.e., in the  $y$  direction in Fig. 1) for the 1D and the two 2D three-loop systems. While not trivial, eventually the transverse gating voltage could be realized experimentally, e.g., by aligning the rings in a thin film or by hooking the rings to gating regions. Interestingly, even a mild gating voltage (0.5 eV) in the  $y$  direction has a very strong effect on the conductance. The reason is that the gating voltage changes the relative phase that the electron gets in the two branches, as will be explained in a simple model later.

The transverse voltages pursued here are relatively mild, up to +0.5 eV, but can be made even smaller by using larger rings; eventually, of course, dephasing effects would start playing a role.

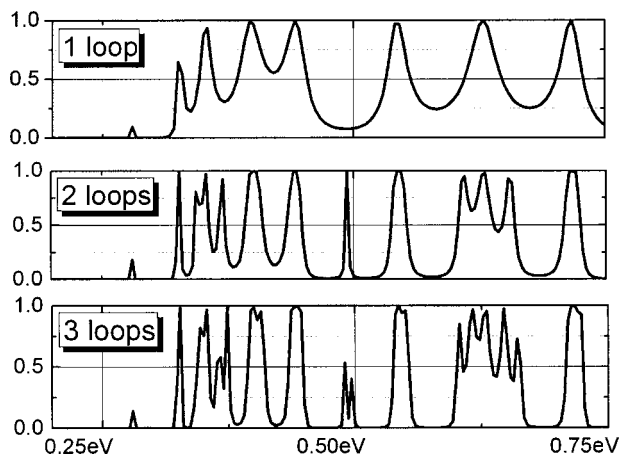


FIG. 3. Analogous to Fig. 2, for a 2D system with a thick bridge.

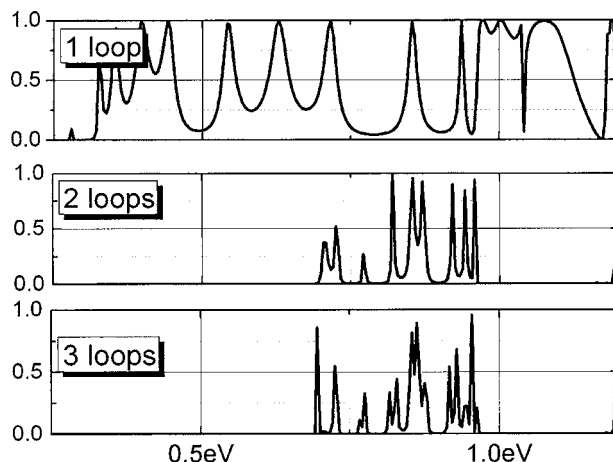


FIG. 4. Analogous to Fig. 2, for a 2D system with a thin bridge.

Gating the bridges in between the rings is another possibility. In some experimental setups it would be more difficult, but it may be easily achieved through substrate gating. Furthermore, if the bridges are sufficiently extended in length it should be even easier to gate them than gating the loops as the bridges are bigger than a nanometer in length. Figures 8–10 show the effects of gating both bridges between the rings for the three-ring case. We studied the effect of gating one bridge (Figs. 8–10), as well as gating both (Fig. 11).

Interestingly, gating can have two sources. It could be due to physically raising the voltage of a gate; alternatively, it could be due to having an incomplete coupling between the loops. This could be, for example, when the loops are manufactured as isolated rings without physical connections, so that the electron has to tunnel between them.

The height and barrier of the tunneling regime has something to do with the precise manufacturing of the loops, so we simulated these effects both by using a variable barrier height (wire gating) and by considering two types of bridges—narrow and thick, as mentioned earlier.

The gating has indeed an effect which is different for positive and negative gateings. For 1D and for the 2D case with thick rings (Figs. 8 and 9), a negative gating changes the structure of the  $N(E)$  vs  $E$  curves. Large effects emerge from a positive gating, which raises the barrier for transmission, and has a very large effect in removing the low-energy bands. However, for the thin-bridge systems (Fig. 10 and

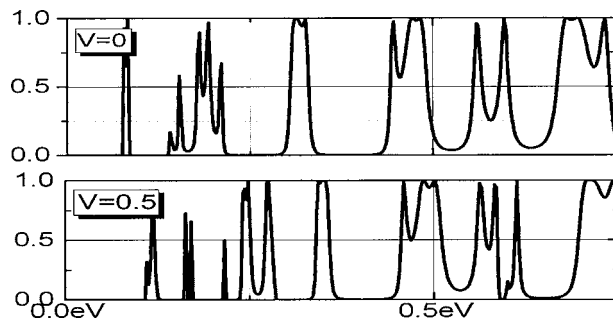


FIG. 5. Transmission vs energy for a 1D system with three loops, showing the effect of applying a transverse voltage of 0.5 eV.

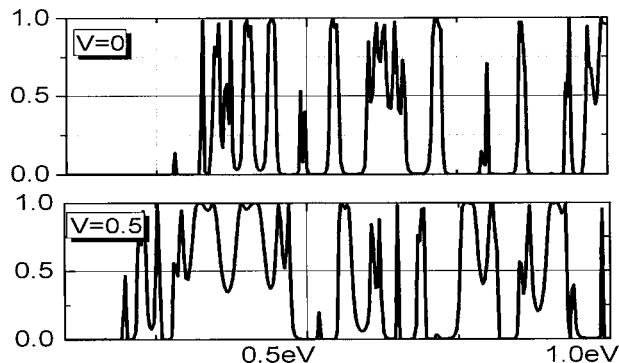


FIG. 6. Analogous to Fig. 5, for a 2D system with three loops and a thick bridge.

especially Fig. 11), the negative gating of the bridges did have large effects, since the small width of the narrow bridges creates an effective barrier which is reduced by the voltage.

Interestingly there is a big difference between a single-bridge gating (Fig. 10) and a two-bridge gating (Fig. 11) for the narrow bridges. When two bridges are gated simultaneously and negatively, narrow resonances appear at low energies; effectively, bound states form on the bridges, which mediate the resonances. In practice, this would mean that if rings are closely placed and are gated in between the rings, then large effects on the transmission are expected.

#### IV. EFFECT OF MAGNETIC FIELD

There are different ways of controlling the phase difference between the coherent propagation of an electron in the rings. In this section, we discuss three ways of controlling the destructive-to-constructive interference in the conduction process: the original Aharonov-Bohm effect due to magnetic fields, the transverse electric field, and the geometrical asymmetry of coupling the ring to the leads. This study is rather qualitative so only a 1D model is used.

##### A. Aharonov-Bohm conductance

Numerical results for the conductance of a 1D single ring for various magnetic-field values are given in Fig. 12.

The easiest way to understand the conductance of a single ring is to consider a model of a 1D ring weakly

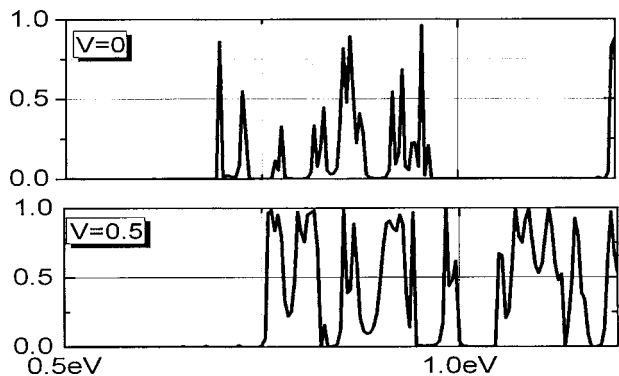


FIG. 7. Analogous to Fig. 5, for a 2D system with three loops and thin bridges.

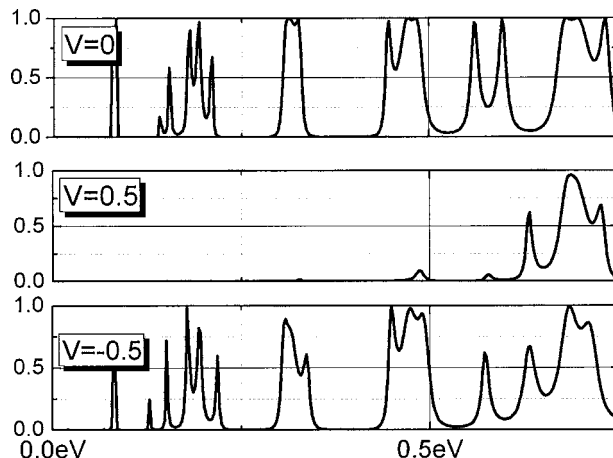


FIG. 8. Transmission vs energy for a 1D system with three loops, showing the effect of applying a gating voltage of 0.5 eV on one of the bridges.

coupled to the left and right 1D wires. The wires are connected to the ring at points  $\varphi=0, \pi$  in polar coordinates, respectively. Since the ring is weakly coupled to the wires, it makes sense to analyze the eigenstates of the electron on the loop alone.

It is natural to measure the magnetic field in units of  $B_0$ , where  $B_0$  is the magnetic field at which the first Aharonov-Bohm blocking of the transmission arises. The Aharonov-Bohm blocking arises when exactly  $1/2$  of the magnetic flux quantum pierces the ring:

$$B_0 = \frac{1}{2} \frac{\Phi_0}{S},$$

where  $S = \pi R^2$  is the 2D area of the ring and  $\Phi_0 = hc/e$  is the magnetic flux quantum. In our numerical studies of the 1D ring system we took  $R = 2.8$  nm, so that  $B_0 = 75$  T is extremely large. However, on a one-particle level all the quantities are scalable and the results obtained apply to bigger systems qualitatively.

The eigenstates of an electron on the ring are enumerated by the angular momentum quantum number  $m = 0, \pm 1, \pm 2, \dots$  and the wave functions are given as

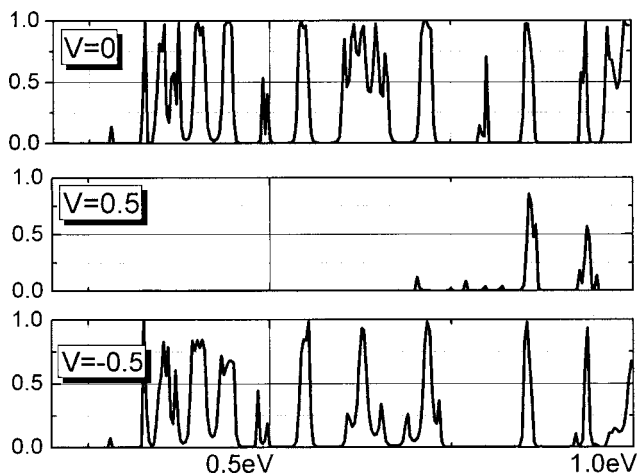


FIG. 9. Analogous to Fig. 8, for a two-dimensional system with three loops and a thick bridge.

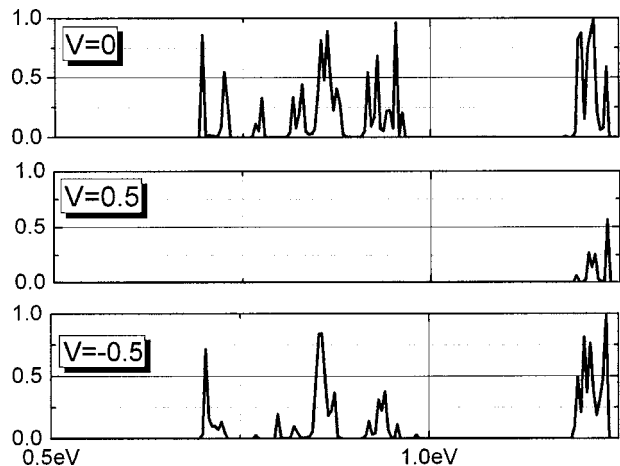


FIG. 10. Analogous to Fig. 8, for a 2D system with three loops and thin bridges.

$$\Psi_m(\varphi) \sim e^{im\varphi}.$$

The energies are given by

$$E_m = \frac{1}{2M} \left( \frac{m}{R} \right)^2,$$

where  $M$  is the electron band mass and  $R$  is the radius of the ring. All the energy levels, except for the one corresponding to the state with  $m=0$ , are doubly degenerate without the magnetic field.

The states may be divided into two groups (see Fig. 13): those coupled to the wires

$$\Psi_{|m|}^c = \frac{1}{\sqrt{2}}(\Psi_m + \Psi_{-m}),$$

and those decoupled from the wires:

$$\Psi_{|m|}^d = \frac{1}{\sqrt{2}}(\Psi_m - \Psi_{-m}).$$

The coupling rate to the wires is proportional to the square of the wave-function modulus at the points of connection to the wires. The decoupled states have nodes at the

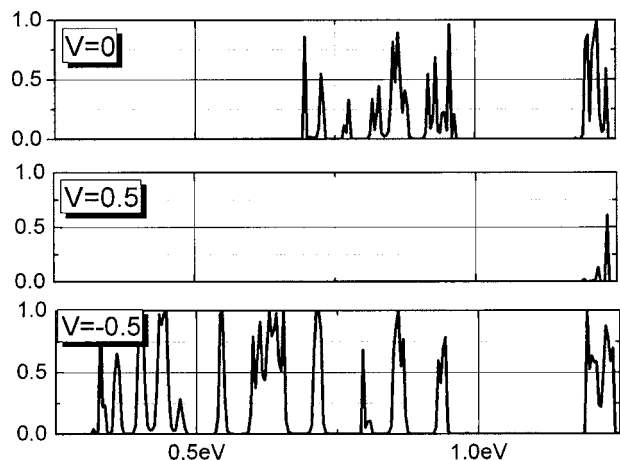


FIG. 11. Transmission vs energy for a 2D system with three loops and thin bridges, showing the effect of applying a gating voltage of  $\pm 0.5$  eV on both bridges.

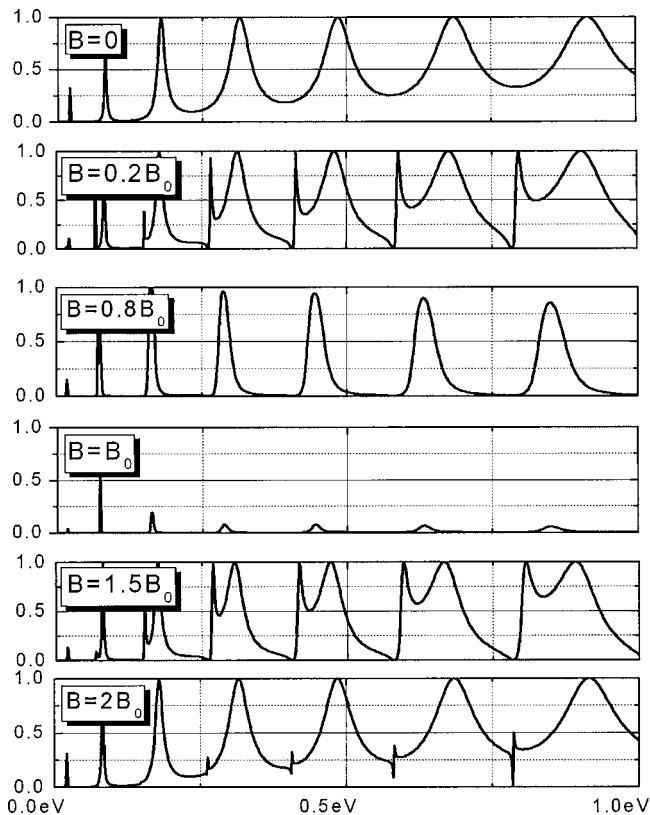


FIG. 12. Transmission vs energy for a 1D system with one loop, showing the effect of applying various magnetic fields on the loops.

points of connection to the rings, which make them “dark” states for electrons coming from and going to the wires. Only the coupled states, which have extrema at the points of connection to the rings, are involved in electron conductance from one wire to the other.

Due to the coupling to the leads, the coupled states obtain widths. The energies of the states are also shifted due to the coupling.

A magnetic field removes the degeneracy of levels with opposite angular momenta  $\pm m$ . A small magnetic field mixes the decoupled states and the continuous density of states of the coupled states. As a result, the decoupled states appear as narrow Fano resonances (Fig. 12 for  $B > 0$ ). As mentioned, the energies of the decoupled and coupled states are different due to the coupling of the latter to the wires.

Then, at larger magnetic fields this picture of the transmission coefficient becomes inconsistent. The transmission coefficient corresponds to equidistant Landau levels.

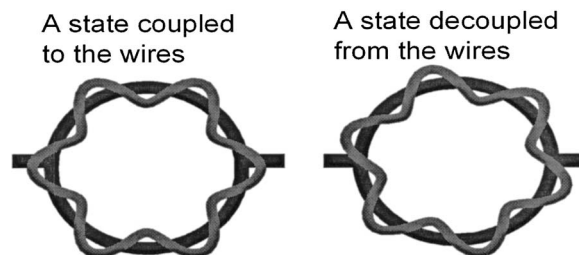


FIG. 13. Schematic representation of the coupled and decoupled states on the ring, discussed in the text.

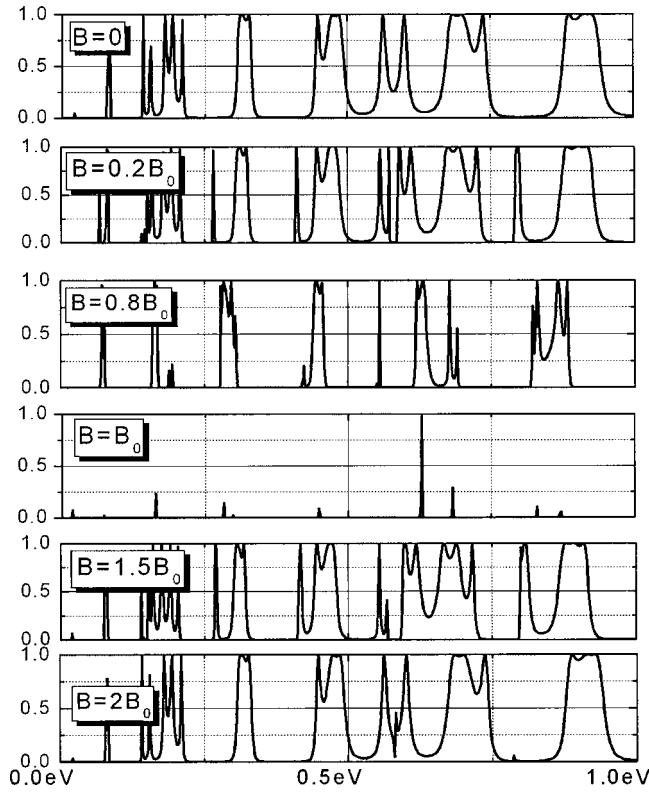


FIG. 14. Transmission vs energy for 1D system with three loops, showing the effect of applying various magnetic fields on the loops.

With further increase of the magnetic field we arrive at the first point of the Aharonov-Bohm blocking of the transmission coefficient for the entire range of the electron energy and/or the chemical potential.

Finally, the transmission coefficient is symmetric with respect to the point of the first Aharonov-Bohm blocking, and also periodic with the period twice larger than the first blocking point.

In Fig. 14, we see again the onset of formation of the band structures from the single-ring conductance in the system of three connected 1D loops.

## B. The effect of transverse electrostatic gating

Imagine now that we applied a transverse electric field to a conducting ring. The upper and lower branches of the wave function of a propagating electron through the ring gain different phases. This should lead to an Aharonov-Bohm-type interference in the conductance coefficient due to the transverse electric field alone.

Consider the situation that there is no magnetic field and a transverse electric field  $E$  is applied. Semiclassically, an additional phase on the upper branch results:

$$\Delta\varphi = R \int d\varphi (\sqrt{2M(\mu + e u R \sin(\varphi))} - \sqrt{2M\mu}).$$

Here,  $R$  is the radius of the ring,  $\mu$  is the chemical potential reckoned from the edge of the electron conduction band, and  $u$  is the electric field.

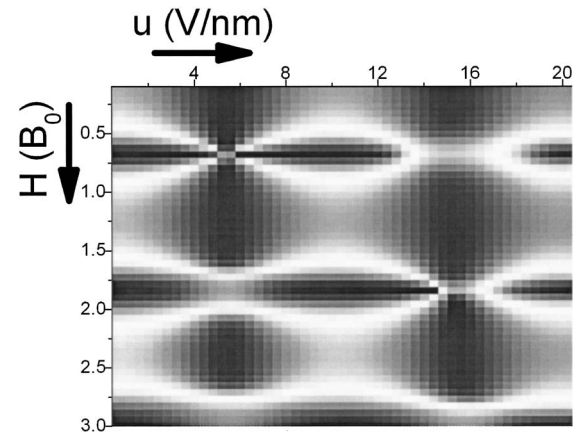


FIG. 15. Transmission coefficient of a 1D single-loop system at a 1-eV electron energy (chemical potential) as a function of magnitudes of the in-plane transverse electric and the out-of-plane magnetic fields.

A reasonable approximation is to assume that the electric potential of the field is smaller than the chemical potential  $\mu$  of the electron. The integration then can be done trivially:

$$\Delta\varphi = eRu \sqrt{\frac{2M}{\mu}}.$$

The additional phase on the lower branch is just  $-\Delta\varphi$ . This means that the transmission coefficient should acquire an oscillation factor:

$$T \propto \left| \cos\left(eRu \sqrt{\frac{2M}{\mu}}\right) \right|^2.$$

Therefore, the effect of an electric field on the phase can be similar to that of a uniform magnetic field, just like in the Aharonov-Bohm theory. Furthermore, it is quite easy to apply an electric field.

Finally, in the case that both magnetic and electric fields are applied, the oscillating factors from Aharonov-Bohm and the transverse electric field appear together and the total oscillation factor in the transmission coefficient reads

$$T \propto \left| \cos\left(\frac{He\pi R^2}{2c}\right) \cos\left(ueR \sqrt{\frac{2M}{\mu}}\right) \right|^2.$$

This formula generalizes the Aharonov-Bohm-type coherent blocking effect for the case that both the out-of-plane magnetic and the transverse in-plane electric fields are applied to the conducting ring. Numerical results for the transmission coefficient at fixed chemical potential 1 eV, and for various magnitudes of both fields, are given in Fig. 15, confirming this formula.

## C. Asymmetric coupling to the leads

Another way of controlling the constructive-to-destructive interference in the conductance through a ring is by exploiting the geometrical asymmetry in the coupling of the ring to the leads. In reality, the wires coupled to the ring are not exactly symmetric. The lengths of the upper and lower arms of a ring are always different. Furthermore, one can deliberately make them different by asymmetric coupling of the leads to a ring.

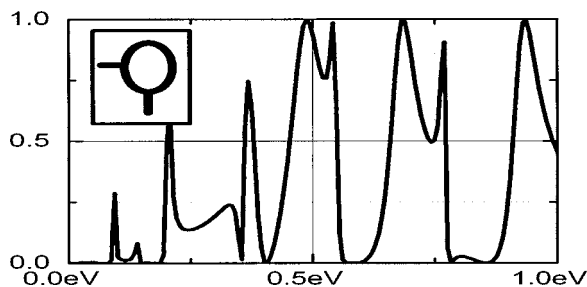


FIG. 16. Transmission vs energy of a 1D one-loop system with asymmetric coupling (as shown on the inset).

In such a case the phase difference between the two paths of the propagation is proportional to the difference between the lengths of the upper and lower paths,  $l_u$  and  $l_l$ , as well as to the wave vector of the propagating electron,  $\Delta\varphi = k(l_u - l_l)$ . The wave vector of the propagating electron is a function of the gating potential. In Fig. 16 we give the results for the transmission probability as a function of energy.

The transmission is a very pronounced function of the electron energy, just like in the case of a magnetic field. Similarly, we also observe Fano-type resonances due to coupling to dark states. We numerically verified that the gating of the loop leads essentially to a shift in the  $T(E)$  vs  $E$  curve, i.e., the transmission is almost a function of  $(E - V_{\text{gating}})$ . So the asymmetric coupled ring behaves similar to the case of a ring in a magnetic field, which raises the hope that an asymmetric coupling to the wires might be exploited for prompt switching of a conducting ring.

## V. CONCLUSION

In conclusion, we have shown that a collection of several quantum rings will have very interesting quantum-mechanical properties. The resonances in the rings are easily tunable, so that the current of electrons passing through can be turned on or off readily, especially if electrons in a narrow energy range are used.

There are several effects that will be studied in future works, including the following:

- The 2D simulations can be made more extensive by doing a closed-coupling approach, which is feasible even if the dots are connected in a direction perpendicular to the motion.
- The transverse voltage was applied here linearly. In practice, of course, one has to solve the Poisson equation to determine the precise potential distribution along the bridges and loops. However, as long as there is a potential drop-off along the bridges, we expect the effect of the gating to persist.
- A further goal is the inclusion of self-consistent effects of currents and their induced magnetic fields.

There are many other possible uses of such devices. First and foremost, it is not necessary to attach the electrons to specific leads; it is feasible to inject the electrons to specific rings using STM tips.

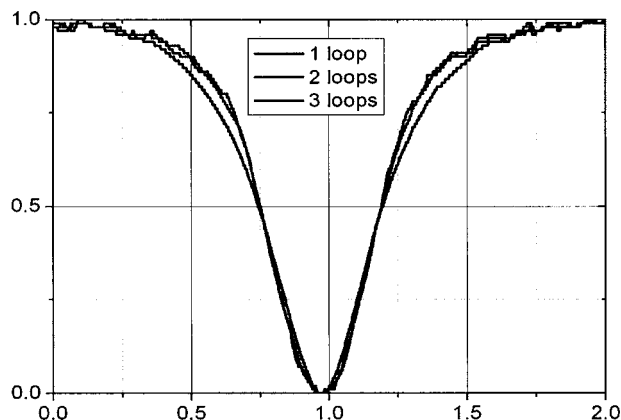


FIG. 17.  $\int N(E)dE$  vs  $B$  for a one-dimensional system with one, two, and three loops.

In addition, a natural aspect of the rings, especially for larger ring sizes, is to examine how a magnetic field changes the spin motion on the rings. For example, if one places incomplete rings so that the electrons are guaranteed to move in a certain direction (clockwise or counterclockwise) and dots the rings with metal ions (to increase spin-orbit interactions), then it is feasible to create spin rings which have different transmission properties for different spins; similar effects are feasible, of course, for regular rings under the presence of magnetic fields, or with the use of spin-orbit interaction, as will be shown in a future work.

Another important property of interference-based ring systems is that since no charging effects are used, the effects of one ring are expected to be isolated from the effects of other ring systems nearby; this will reduce long-range effects that can complicate the use of charging in dots for computations.

## ACKNOWLEDGMENTS

We thank NSF, PRF, and the UCLA office of the Dean for supporting this research.

- <sup>1</sup>J. Rose and D. Baugh, Appl. Phys. Lett. (submitted).
- <sup>2</sup>J. Rose and D. Baugh, Mater. Res. Soc. Symp. Proc. (in press).
- <sup>3</sup>A. B. Fowler, U.S. Patent No. 4,550,330 (1984).
- <sup>4</sup>K. Walczak, Cent. Eur. J. Chem. **2**, 524 (2004).
- <sup>5</sup>F. Guinea, Phys. Rev. B **65**, 205317 (2002).
- <sup>6</sup>Z. Barticevic, G. Fuster, and M. Pacheco, Phys. Rev. B **65**, 193307 (2002).
- <sup>7</sup>G. Bergamini *et al.*, J. Am. Chem. Soc. **126**, 16466 (2004).
- <sup>8</sup>K. P. Ghiggino *et al.*, J. Incl. Phen. and Macr. Chem. **49**, 27 (2004).
- <sup>9</sup>V. Krishna *et al.*, J. Am. Chem. Soc. **113**, 3325 (1991).
- <sup>10</sup>O. Hod, R. Baer, and E. Rabani, J. Phys. Chem. B **108**, 14807 (2004); J. Am. Chem. Soc. **127**, 1648 (2005).
- <sup>11</sup>S. Datta, *Electronic Transport in Mesoscopic Systems* (Cambridge University Press, Cambridge, 1995).
- <sup>12</sup>A. Lorke *et al.*, Phys. Rev. Lett. **84**, 2223 (2000).
- <sup>13</sup>J. P. Colinge, *Si-on-Insulator Technology: Materials to VLSI* (Kluwer, Dordrecht, 1991).
- <sup>14</sup>T. Seideman and W. H. Miller, J. Chem. Phys. **97**, 2499 (1992).
- <sup>15</sup>D. Neuhauser and M. Baer, J. Chem. Phys. **93**, 7836 (1990).
- <sup>16</sup>D. T. Colbert and W. H. Miller, J. Chem. Phys. **96**, 1982 (1992).
- <sup>17</sup>D. J. Griffiths and C. A. Steinke, Am. J. Phys. **69**, 137 (2001).